

2012

# Displacement-based two-finger grasping of deformable planar objects

Feng Guo

*Iowa State University*

Follow this and additional works at: <https://lib.dr.iastate.edu/etd>



Part of the [Computer Sciences Commons](#), and the [Robotics Commons](#)

---

## Recommended Citation

Guo, Feng, "Displacement-based two-finger grasping of deformable planar objects" (2012). *Graduate Theses and Dissertations*. 12648.  
<https://lib.dr.iastate.edu/etd/12648>

This Thesis is brought to you for free and open access by the Iowa State University Capstones, Theses and Dissertations at Iowa State University Digital Repository. It has been accepted for inclusion in Graduate Theses and Dissertations by an authorized administrator of Iowa State University Digital Repository. For more information, please contact [digirep@iastate.edu](mailto:digirep@iastate.edu).

**Displacement-based two-finger grasping of deformable planar objects**

by

Feng Guo

A thesis submitted to the graduate faculty  
in partial fulfillment of the requirements for the degree of  
MASTER OF SCIENCE

Major: Computer Science

Program of Study Committee:

Yan-Bin Jia, Major Professor

Vasant Honavar

James Oliver

Iowa State University

Ames, Iowa

2012

Copyright © Feng Guo, 2012. All rights reserved.

## DEDICATION

I would like to dedicate this thesis to my wife Yueran Yang and my parents without whose support I would not have been able to complete this work.

## TABLE OF CONTENTS

<b>LIST OF TABLES</b> . . . . .	v
<b>LIST OF FIGURES</b> . . . . .	vi
<b>ACKNOWLEDGEMENTS</b> . . . . .	vii
<b>ABSTRACT</b> . . . . .	viii
<b>CHAPTER 1. INTRODUCTION</b> . . . . .	1
1.1 Assumptions . . . . .	2
1.2 The Grasping Problem . . . . .	3
1.3 Thesis Outline . . . . .	4
<b>CHAPTER 2. REVIEW OF LITERATURE</b> . . . . .	5
<b>CHAPTER 3. FINITE ELEMENT METHOD</b> . . . . .	6
3.1 Linear Plane Elasticity . . . . .	6
3.2 Stiffness Matrix . . . . .	8
<b>CHAPTER 4. TWO FINGER SQUEEZE</b> . . . . .	11
4.1 Deformation due to Contact Displacement . . . . .	12
4.2 Squeeze Grasp . . . . .	16
4.3 Generalized Squeeze Grasp . . . . .	18
<b>CHAPTER 5. GRASP COMPUTATION</b> . . . . .	20
5.1 An Efficient Algorithm . . . . .	21
5.2 Algorithm Analysis . . . . .	23
<b>CHAPTER 6. ROBOT EXPERIMENT</b> . . . . .	25
<b>CHAPTER 7. DISCUSSION</b> . . . . .	29

**BIBLIOGRAPHY** ..... 30

**LIST OF TABLES**

Table 5.1	Algorithm Comparison . . . . .	24
Table 6.1	Grasping Two Ring-like Objects . . . . .	26

## LIST OF FIGURES

Figure 1.1	Squeeze Grasp . . . . .	3
Figure 3.1	Planar Object . . . . .	6
Figure 3.2	Rotation Field under Linear Elasticity . . . . .	8
Figure 3.3	Triangular Mesh . . . . .	9
Figure 4.1	Translation of $\mathbf{p}_i$ towards $\mathbf{p}_0$ . . . . .	12
Figure 4.2	Generalized Squeeze Grasp . . . . .	19
Figure 6.1	Grasping with a Barrett Hand. . . . .	25
Figure 6.2	Graspable regions . . . . .	27
Figure 6.3	Independent Grasp Region . . . . .	28
Figure 6.4	Grasping a Foam Object . . . . .	28

## ACKNOWLEDGEMENTS

I would like to take this opportunity to express my thanks to people who gave me all kinds of help in my study.

First and foremost, I would like to thank Dr. Yan-Bin Jia, who has given me tremendous support, inspiring guidance and valuable help on my research. It was such a pleasure to work with him during the Master's career. He has always been there when I have difficulties in research and guide me towards a thinker.

I am also greatly thankful to my committee members, Dr. Vasant Honavar and Dr. James Oliver, for their help and contribution to this work. It is such an honor to have them as my committee member and learn from them.

The Robotics Lab has been a great place for study and research. All the lab members in the lab, Jiang Tian, HyunTae Na, Theresa Driscoll, Huan Lin, Rex Fernando, Feifei Wang and Sean Strickland, have made it a lovely place. I am grateful to them all.

I would also thank other friends Yetian Chen, Ru He, Chuan Jiang, Tsing-yi Jiang, Zi Li, Lisen Peng, Yang Peng, Hua Qin, Chuang Wang, Wanwu Wang, Liyuan Xiao, Jinsheng Zhang, Wei Zhang. Their presences make Ames a lovely home to me.

Support for this research has been provided in part by Iowa State University, and in part by the National Science Foundation through the grant IIS-0915876. Any opinions, findings and conclusions or recommendations in this thesis are those of the author and do not necessarily reflect the views of the National Science Foundation



**ABSTRACT**

This thesis introduces a strategy of grasping deformable objects using two fingers which specifies finger displacements rather than grasping forces. Grasping deformable objects must maintain its equilibrium before and after the induced deformation. The deformed shape and grasping force are computed using the finite element method (FEM). The equilibrium of the object is guaranteed automatically since the computed grasping force are collinear and sum up to 0. To achieve a grasp, the forces have to be tested for staying inside the pre- and post-deformation contact friction cones. This test could be as expensive as solving a large linear system, if the deformed shape is computed. We present an algorithm that performs a grasp test in  $O(n)$  time, where  $n$  is the number of discretization vertices under FEM, after obtaining the spectral decomposition of the object's stiffness matrix in  $O(n^3)$  time. All grasps (up to discretization) can be found in additional  $O(n^2)$  time. Robot grasping experiments have been conducted on thin  $2\frac{1}{2}$ D objects.

## CHAPTER 1. INTRODUCTION

Grasping deformable objects is quite different from grasping rigid ones. Two types of analysis have been developed for the latter. Form closure means the object cannot move given the fingers are fixed, while force closure grasps resist any arbitrary wrench and keep the object in equilibrium. However, deformable objects have infinite degrees of freedom, which makes form closure impossible. On the other hand, the grasp wrench space changes as the object deforms, which makes it impossible to conduct any conventional force closure analysis.

Deformable objects are very common in our world. However grasping of deformable objects is an under-researched area, primarily due to the following reasons. Physics-based deformation modeling is computationally expensive, but necessary since deformation is involved. Besides, the grasped object must be in equilibrium at more than one scenario: before and after deformation.

The deformation induced by a grasp can be modeled using the elasticity theory, in which the applied force and the displacement of the contact are strictly related and thus cannot be both specified at the same time. In this thesis, we choose to specify desired displacements of the fingers rather than the force exerted, for the following reasons:

1. In practice, it is much easier to control the finger's displacement than the force it exerted. Controlling the robotic hands' movement or locations is by far the most common, direct, easy way of manipulation.
2. The exact grasping force, especially that in deformation process, is not very much concerned, as long as the object can be grasped.
3. Specifying the displacement gives rise to certain constraints that are sufficient for determining the deformation and corresponding force.

Linear elasticity is applicable when the deformation is small enough. Computation of deformed shape based on linear elasticity comes down to solving either a system of fourth order differential equations, which has no closed-form solution in general, or practically, a large linear system using Finite Element Method(FEM). The latter takes subcubic time in the number of discretization nodes, which is typically high for accurate modeling. A large deformation can only be modeled by nonlinear elasticity and computed using the even more expensive nonlinear FEM.

The lack of a closed form description of the deformed shape implies that (part of) the shape needs to be computed repeatedly with hypothesized finger placements in order to compute a single grasp. Computational efficiency has thus become a bottleneck, even more so for grasp optimization and real-time implementation.

Whether a finger placement with certain finger displacement can form a grasp without slip depends on the local geometry of the contacts. Therefore global deformation is not needed. The stiffness matrix of the object stays the same for different grasp tests, although the boundary conditions may vary. An improvement in computation is possible by preprocessing the stiffness matrix.

## 1.1 Assumptions

In this thesis, we focus on how to grasp planar objects without concerning any body force, e.g. gravity. The contacts between fingers and objects are point contacts with friction. The object deforms with finger's displacement. When the deformation is small enough, linear elasticity theory applies. Classical elasticity theory often ignores dynamics in modeling deformation. So the following assumptions are made.

(A1) The object to be grasped is isotropic, and either planar or thin  $2\frac{1}{2}$ D.

(A2) Gravity is ignored as the object lies in a horizontal supporting plane.

(A3) Two grasping fingers are in the same plane, and make point contacts with the object in the presence of friction.

- (A4) The deformation yielded by a grasp is small enough so that the linear elasticity theory is applicable.
- (A5) Deformation happens instantaneously such that the applied contact forces do not vary, and no velocity of the object builds up.

## 1.2 The Grasping Problem

Figure 1.1 shows a grasp achieved by squeezing an object. The action is equivalent to keeping one finger still and stuck to its contact point, say,  $\mathbf{q}$ , while translating the other finger toward  $\mathbf{q}$  without slip at its contact point  $\mathbf{p}$ .

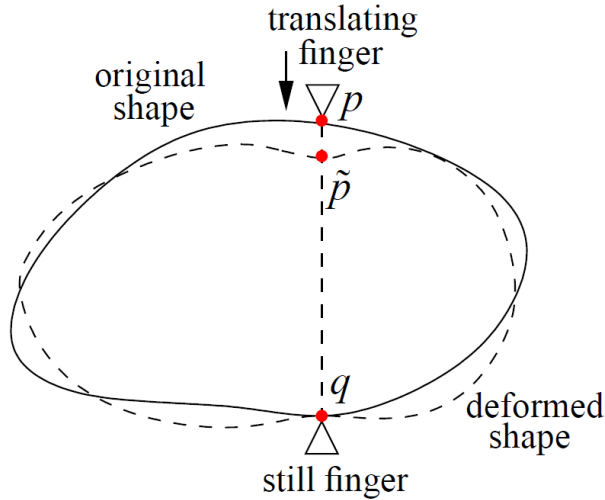


Figure 1.1: Squeeze Grasp

To grasp the deformable object in Figure 1.1, the finger placement  $\mathcal{G}(\mathbf{p}, \mathbf{q})$  should prevent any Euclidean motion such that the only possible displacement is deformation. In presence of friction, this requires the grasp to be force closure if the object were rigid. By Nguyen's result (13), the segment  $\overline{\mathbf{p}\mathbf{q}}$  in Figure 1.1 must lie inside the friction cones at  $\mathbf{p}$  and  $\mathbf{q}$  on the object's original shape.

If no contact slips, the same finger placement exerting the same forces also needs to maintain equilibrium over the deformed shape of the object. Suppose under the deformation the contact points  $\mathbf{p}$  and  $\mathbf{q}$  have moved to  $\tilde{\mathbf{p}}$  and  $\tilde{\mathbf{q}}$ , resp. The segment  $\overline{\tilde{\mathbf{p}}\tilde{\mathbf{q}}}$  must lie inside the friction cones at  $\tilde{\mathbf{p}}$  and  $\tilde{\mathbf{q}}$  on the object's post-deformation shape.

### 1.3 Thesis Outline

This thesis will formally characterize squeeze grasps like the one shown in Figure 1.1, and describe an efficient algorithm to compute them. Chapter 2 reviews the related research that has been done. Chapter 3 will briefly review linear elasticity and FEM with derivations of some basic results to be used later. In Chapter 4, we will show that it is possible to grasp a deformable object by squeezing it with two fingers moving toward each other along a straight line, as long as the connection line of the two contacts stay inside the contact friction cones before and after deformation. We will also show that actions other than pure squeeze can also result in grasps if so does the corresponding pure squeeze. Chapter 5 will present an  $O(n)$  time algorithm for grasp testing, where  $n$  is the number of vertices in FEM, after obtaining the singular value decomposition (SVD) of the object's stiffness matrix. The cost of finding all grasps reduces to  $O(n^2)$ . It turns out that SVD, which takes  $O(n^3)$  time, dominates the overall computation. Chapter 6 will present experiments on grasping ring-like and solid 2-D objects using a Barrett Hand. Discussion on future research will follow in Chapter 7 to conclude the thesis.

## CHAPTER 2. REVIEW OF LITERATURE

Rigid body grasping is an extensively studied area rich with theoretical analyses, algorithmic syntheses, and implementations with robotic hands (1). In particular, two-finger force-closure grasps of 2-D objects are well understood and efficiently computable for polygons (13) and piecewise-smooth curved shapes (15).

Much fewer work exists on grasping of deformable objects, which needs to deal with accurate modeling of deformations caused by the grasping forces. In (16), a model for deformable contact regions under a grasp was introduced to predict normal and tangential contact forces with no concern of grasp computation or modeling of global deformation. Simulation accuracy and efficiency could be improved based on derived geometric properties at deformable contact (10). Deformation modeling of shell-like objects that have been grasped is studied in (18).

The concept of bounded force-closure was proposed in (19). Visual and tactile information was effective on controlling the motion of a grasped deformable object (7). The deformation-space (D-space) approach (6) characterized the optimal grasp of a deformable part as one where the potential energy needed to release the part equals the amount needed to squeeze it to its elastic limit— hence the object could not escape.

The recent work (9) specifies grasping forces instead of finger displacements. Extra constraints, which lead to unrealistic requirements, had to be imposed for computing the deformed shape. The corresponding grasp space (i.e., the set of feasible finger placements) was 1-D, and the synthesis algorithm was too inefficient to be applicable to solid 2-D objects.

## CHAPTER 3. FINITE ELEMENT METHOD

The first part of this chapter reviews the 2D linear elasticity. The displacement field which does not generate strain energy is characterized. The second part describes the Finite Element Method used to model the deformation. The null space of the stiffness matrix is shown. The result will later be used in our design of a grasping strategy.

### 3.1 Linear Plane Elasticity

Consider a thin flat object as is shown in Figure 3.1, the thickness  $h$  of which is dominated by the other two dimensions. The object is bounded by a generalized cylinder. Here we consider the *plane stress* (4) parallel to the  $xy$ -plane, which assumes zero normal stress  $\sigma_z$  and shear stresses  $\tau_{xz}$  and  $\tau_{yz}$  in the  $xz$  and  $yz$  planes.

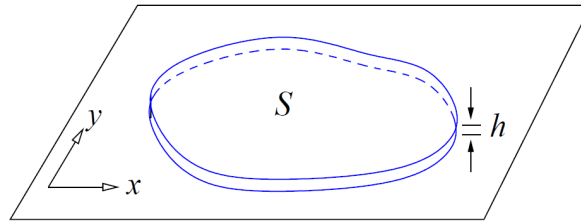


Figure 3.1: Planar Object

Under a displacement field  $(u(x, y), v(x, y))$ , every point of the object moves to  $(x+u, y+v)$ . The normal strains  $\varepsilon_x$ ,  $\varepsilon_y$  and the shearing strain  $\gamma_{xy}$  within every cross section are given below:

$$\begin{aligned}
 \varepsilon_x &= \frac{\partial u}{\partial x}, \\
 \varepsilon_y &= \frac{\partial v}{\partial y}, \\
 \gamma_{xy} &= \frac{\partial u}{\partial y} + \frac{\partial v}{\partial x}.
 \end{aligned} \tag{3.1}$$

The strain energy can be derived as (3):

$$U = \frac{h}{2} \iint_S \left( \frac{E}{1-v^2} (\varepsilon_x^2 + 2v\varepsilon_x\varepsilon_y + \varepsilon_y^2) + \frac{E}{2(1+v)} \gamma_{xy}^2 \right) dx dy, \quad (3.2)$$

where  $E$  and  $v$  are Young's modulus and Poisson's ratio of the material, resp., with  $E > 0$  and  $-1 \leq v \leq \frac{1}{2}$ .

**Theorem 1.** *Under linear elasticity, any displacement field  $(u(x, y), v(x, y))$  that yields zero strain energy is linearly spanned by three fields:  $(1, 0)$ ,  $(0, 1)$  and  $(-y, x)$ .<sup>1</sup>*

*Proof.* Suppose  $U = 0$  under a displacement field  $(u, v)$ . From 3.2 we see that the strains  $\varepsilon_x$ ,  $\varepsilon_y$  and  $\gamma_{xy}$  must vanish everywhere. From 3.1,

$$\begin{aligned} u &= \int \varepsilon_x dx + f(y) = \int 0 dx + f(y) = f(y), \\ v &= \int \varepsilon_y dy + g(x) = \int 0 dy + g(x) = g(x), \end{aligned}$$

where  $f$  and  $g$  are arbitrary single variable functions. Since  $\gamma_{xy} = 0$ ,  $du/dy + dv/dx = f'(y) + g'(x) = 0$  for all  $(x, y)$  in the body. Given  $f$  and  $g$  do not share variable,  $f'(y) = -g'(x) = c$  for some constant  $c$ . Integration of the two derivatives gives

$$(u, v) = c(-y, x) + d(1, 0) + e(0, 1),$$

for some constants  $d$  and  $e$ . □

Displacement fields that generate no strain energy are essentially rigid body transformations. The fields  $(1, 0)$  and  $(0, 1)$  represent translation in  $x$ - and  $y$ - directions resp. The field  $(-y, x)$ , which displays every point  $(x, y)$  in the direction orthogonal to  $(x, y)$ , corresponds to rotation around origin. Note that, as is shown in Figure 3.2, it approximates rotation well only when the rotation is small enough. When it is not, such field also inflates the original shape. When such field is large enough, the change of the orientation of the object approaches  $\pi/2$ . Such deviation from the real rotation indicates certain limit of linear elasticity in modeling the real world.

---

<sup>1</sup>Theorem given and proven by Yan-Bin Jia.



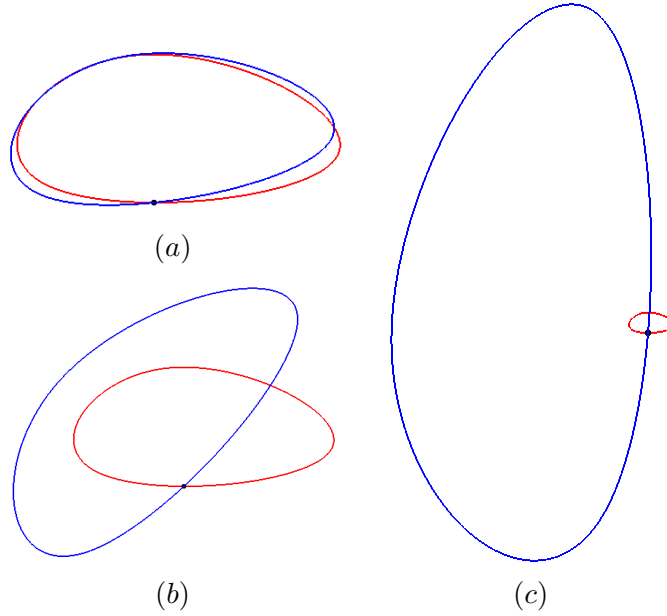


Figure 3.2: The rotation field under linear elasticity. The red shape is original shape, while the blue one shows the shape under certain rotation field. Denote the original shape as  $S$  and the rotation field as  $r$ , the blue shapes can be expressed as  $S + \lambda r$ , where  $\lambda$  is a real number. (a),(b) and (c) show the resulting shape when  $\lambda$  is very small, certain value that is note very small and approaching infinity, resp. (b) and (c) are shrunk to fit.

### 3.2 Stiffness Matrix

For the rest part of the paper, all vectors are column vectors and all indices in a vector or matrix start at 0.

Closed forms of the strain energy integrals do not exist for most objects. The Finite Element Method(FEM) is widely used to compute it (and the deformation). The object's cross section is discretized into a finite number of elements(e.g. triangles) with vertices  $\mathbf{p}_0, \dots, \mathbf{p}_{n-1}$ , where  $\mathbf{p}_k = (p_{kx}, p_{ky})^T$ , for  $0 \leq k \leq n - 1$ . Among these vertices,  $\mathbf{p}_0, \dots, \mathbf{p}_{m-1}$  where  $m \leq n$ , are on the boundary in counterclockwise order. One example is shown in Figure 3.3.

Let  $\Delta = (\delta_0^T, \dots, \delta_{n-1}^T)^T$ , where  $\delta_k = (\delta_{kx}, \delta_{ky})^T$ , be the displacement of  $\mathbf{p}_k$ , for  $0 \leq k \leq n - 1$ , the displacement of any interior point of an element can be linearly interpolated over those of the vertices of the element. The displacement field and the deformed shape are thus uniquely determined by  $\Delta$ . We first obtain the strain energies of individual elements, and then

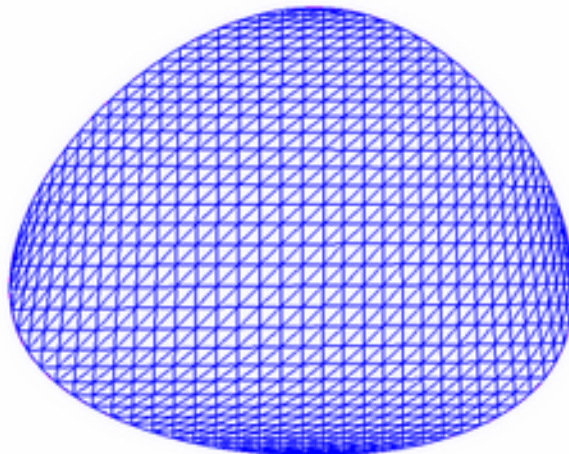


Figure 3.3: Triangular mesh with 3,120 vertices, 156 of which are on the boundary.

assemble them into the total strain energy:

$$U = \frac{1}{2} \Delta^T K \Delta, \quad (3.3)$$

where  $K$  is the  $2n \times 2n$  *stiffness matrix*. The fact that  $K$  is quadratic form indicates the symmetry of  $K$ , and the non-negativeness of strain energy ensures that  $K$  is positive semi-definite.

The strain energy  $U$  is zero if and only if  $K\Delta = 0$ , that is,  $\Delta$  is in the null space of  $K$ . Such a vector  $\Delta$  gives the form of a rigid body displacement (5, pp. 48). Meanwhile, by Theorem 1, the displacement field generating zero strain energy is spanned by  $(-y, x)$ ,  $(0, 1)$  and  $(1, 0)$ . Under linear interpolation, it indicates that the null space of  $K$ , where lies  $\Delta$ , is spanned by the following three vectors:

$$\mathbf{v}_x = \begin{pmatrix} 1 \\ 0 \\ \vdots \\ 1 \\ 0 \end{pmatrix}, \quad \mathbf{v}_y = \begin{pmatrix} 0 \\ 1 \\ \vdots \\ 0 \\ 1 \end{pmatrix}, \quad \mathbf{v}_r = \begin{pmatrix} -p_{0y} \\ p_{0x} \\ \vdots \\ -p_{n-1,y} \\ p_{n-1,x} \end{pmatrix}. \quad (3.4)$$

Here  $\mathbf{v}_x$  and  $\mathbf{v}_y$  translate all vertices by unit distance in the  $x$ - and  $y$ -directions, resp., while  $\mathbf{v}_r$  rotates them about the origin. Note that  $\mathbf{v}_r$  is orthogonal to  $\mathbf{v}_x$  and  $\mathbf{v}_y$  if the geometric center of the object is placed at origin.

**Lemma 1.** *The stiffness matrix  $K$  of an (unconstrained) object with  $n$  discretization vertices has rank  $2n - 3$ .*

Following from Lemma 1, the matrix  $K$  has  $2n - 3$  positive eigenvalues  $\lambda_0, \dots, \lambda_{2n-4}$ . Let  $\mathbf{u}_0, \dots, \mathbf{u}_{2n-4}$  be the corresponding unit eigenvectors, and

$$\begin{aligned}\mathbf{u}_{2n-3} &= \frac{\mathbf{v}_x}{\|\mathbf{v}_x\|}, \\ \mathbf{u}_{2n-2} &= \frac{\mathbf{v}_y}{\|\mathbf{v}_y\|}, \\ \mathbf{u}_{2n-1} &= \frac{\mathbf{z}}{\|\mathbf{z}\|}.\end{aligned}\tag{3.5}$$

where  $\mathbf{z} = \mathbf{v}_r - (\mathbf{v}_r \cdot \mathbf{u}_{2n-3})\mathbf{u}_{2n-3} - (\mathbf{v}_r \cdot \mathbf{u}_{2n-2})\mathbf{u}_{2n-2}$ , correspond to the zero eigenvalues. It follows from the Spectral Theorem (17) that

$$K = U\Lambda U^T,\tag{3.6}$$

where  $U = (\mathbf{u}_0, \dots, \mathbf{u}_{2n-1})$  is orthonormal, and  $\Lambda = \text{diag}(\lambda_0, \dots, \lambda_{2n-4}, 0, 0, 0)$ .

Suppose the object is in equilibrium with the configuration  $(\Delta, \mathbf{F})$ . Since only boundary vertices take external force,  $\mathbf{F} = (\mathbf{f}_0^T, \dots, \mathbf{f}_{m-1}^T, 0, \dots, 0)^T$ . According to Virtual Work Principle (5, pp. 136), the *virtual work* done by the equilibrium force  $\mathbf{F}$  through a *virtual displacement*<sup>2</sup> is equal to the change of potential energy of the object under such virtual displacement, which leads to

$$K\Delta = \mathbf{F}.\tag{3.7}$$

In Equation 3.7, we have  $4n$  variables,  $2n$  from  $\Delta$  and  $2n$  from  $\mathbf{F}$ , and we need half of them to be known to solve for the other half. Note that since  $K$  is singular, if improper variables are picked as known, for example, the  $2n$  variables of  $\mathbf{F}$ , we will get a space of the unknown variables rather than a specific solution. In the next chapter, constraints generated by the grasping strategy will be imposed so that the solution to the system is unique.

---

<sup>2</sup>The virtual displacement is an admissible imaginary infinitesimal displacement that is superposed to the equilibrium deformation.

## CHAPTER 4. TWO FINGER SQUEEZE

As shown in Figure 4.1, we place two fingers at  $\mathbf{p}_0$  and  $\mathbf{p}_i$ . The finger at  $\mathbf{p}_0$  is kept still, while the other finger at  $\mathbf{p}_i$  squeezes the object for a grip. Without loss of generality, we place  $\mathbf{p}_0$  at the origin and align the positive  $y$ -axis with  $\overrightarrow{\mathbf{p}_0\mathbf{p}_i}$ . The remaining boundary points are not in contact with anything, thus no forces are applied. So

$$\mathbf{f}_k = 0, \tag{4.1}$$

for  $1 \leq k \leq n - 1$  with  $k \neq i$ . The force vector is now

$$\mathbf{F} = \begin{pmatrix} \mathbf{f}_0 \\ 0 \\ \vdots \\ 0 \\ \mathbf{f}_i \\ 0 \\ \vdots \\ 0 \end{pmatrix}. \tag{4.2}$$

**Proposition 1.** *The forces exerted by the two fingers are opposite to each other, that is,  $\mathbf{f}_0 + \mathbf{f}_i = 0$ .*

*Proof.* Since  $\mathbf{v}_x$  and  $\mathbf{v}_y$  are in the null space of  $K$ , they are orthogonal to the eigenvectors corresponding to non-zero eigenvalues. Substitute Equation 3.6 into 3.7,

$$U\Lambda U^T \Delta = \mathbf{F}. \tag{4.3}$$

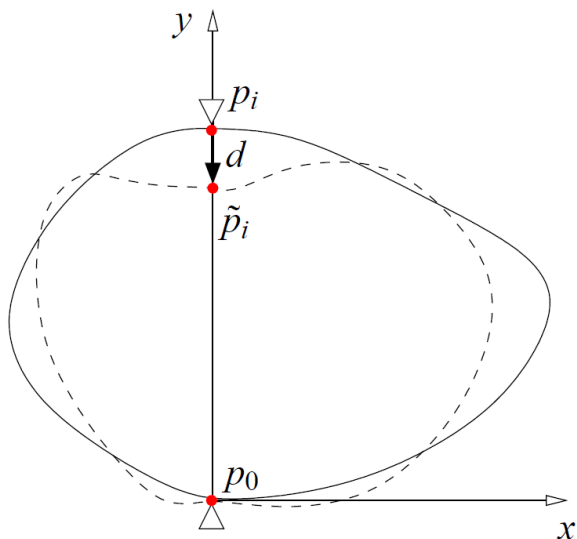


Figure 4.1: Translation of  $\mathbf{p}_i$  towards  $\mathbf{p}_0$ .

Left multiply  $\mathbf{v}_x^T$  on both sides of the above equation and substitute Equation 4.2 in, the left side vanishes, yielding

$$0 = (1, 0, \dots, 1, 0) \begin{pmatrix} \mathbf{f}_0 \\ 0 \\ \vdots \\ 0 \\ \mathbf{f}_i \\ 0 \\ \vdots \\ 0 \end{pmatrix},$$

or equivalently,  $(1, 0) \cdot (\mathbf{f}_0 + \mathbf{f}_i) = 0$ . Similarly, multiplications of  $\mathbf{v}_y^T$  on Equation 4.3 lead to  $(0, 1) \cdot (\mathbf{f}_0 + \mathbf{f}_i) = 0$ . Thus we have  $\mathbf{f}_0 + \mathbf{f}_i = 0$ .  $\square$

From now on, we will write  $\mathbf{f}_0 = -\mathbf{f}$  and  $\mathbf{f}_i = \mathbf{f}$ .

#### 4.1 Deformation due to Contact Displacement

Squeezing the object is possible if

- 1) the two fingers can maintain its equilibrium before and after the deformation that would result from such a squeeze, and
- 2) no slip happens at either finger contact.

Our strategy is to first look at how the object deforms under constraints that assume condition 2, and then verify the consistency between both conditions and the computed deformation under them.

The stationary finger in contact with the object at  $\mathbf{p}_0$  indicates

$$\delta_0 = 0. \quad (4.4)$$

This eliminates  $\mathbf{v}_x$  and  $\mathbf{v}_y$  from the solution space of Equation 3.7 because translations are now prohibited. The vector, now with  $p_{0x} = p_{0y} = 0$ , represents a rotation about  $\mathbf{p}_0$ —the only rigid body motion left. In Equation 3.7, we eliminate the first two rows and columns from  $K$ , and the first two elements each from  $\Delta$  and  $\mathbf{F}$ , obtaining

$$K' \Delta' = F', \quad (4.5)$$

where  $\Delta' = (\delta_1^T, \dots, \delta_{n-1}^T)$  and  $F' = (0, \dots, 0, \mathbf{f}^T, 0, \dots, 0)^T$ . The null space of  $K'$  is spanned by the vector<sup>1</sup>

$$\mathbf{v}_r = \begin{pmatrix} -p_{1y} \\ p_{1x} \\ \vdots \\ -p_{n-1,y} \\ p_{n-1,x} \end{pmatrix}. \quad (4.6)$$

The  $(2n - 2) \times (2n - 2)$  matrix  $K'$  is symmetric and positive semi-definite, with rank  $2n - 3$ , and can be spectrum-decomposed as:

$$K' = \sum_{i=0}^{2n-3} \lambda'_i \mathbf{u}'_i \mathbf{u}'_i{}^T, \quad (4.7)$$

where  $\lambda'_i$ 's are eigenvalues of  $K'$  with  $\lambda'_{2n-3} = 0$ , and  $\mathbf{u}'_i$ 's are corresponding eigenvectors, with  $\mathbf{u}'_{2n-3} = \mathbf{v}'_r / \|\mathbf{v}'_r\|$ .

---

<sup>1</sup>Note that  $p_{ix} = 0$  in the coordinate system in Figure 4.1.

**Proposition 2.** *The contact force  $\mathbf{f}$  exerted at  $\mathbf{p}_i$  under constraint 4.4 is collinear with the segment  $\overline{\mathbf{p}_0\mathbf{p}_i}$ .*

*Proof.* Like what we do in proving Proposition 1, we substitute Equation 4.7 into 4.5, and multiply both sides of the resulting equation with  $\mathbf{u}'_{2n-3}$ , obtaining

$$0 = \mathbf{u}'_{2n-3}{}^T \mathbf{F}',$$

or equivalently,  $\mathbf{v}'_r{}^T \mathbf{F}' = 0$ , which by Equation 4.6 reduces to  $(-p_{iy}, p_{ix})\mathbf{f} = 0$ . Thus  $\mathbf{f}$  and  $\overline{\mathbf{p}_0\mathbf{p}_i}$  are colinear.  $\square$

Under Proposition 2, we conveniently represent the squeezing force exerted by the moving finger as  $\mathbf{f} = (0, -f)^T$  with  $f$  being its magnitude. So

$$\mathbf{F}' = \begin{pmatrix} 0 \\ \vdots \\ 0 \\ -f \\ 0 \\ \vdots \\ 0 \end{pmatrix},$$

where the entry  $-f$  has index  $2i - 1$ .

As an important part of our strategy, we specify the finger displacement. Such specification gives us another boundary condition:

$$\delta_i = \mathbf{d} = \begin{pmatrix} d_x \\ d_y \end{pmatrix}. \quad (4.8)$$

Rewrite  $\Delta'$  as

$$\Delta' = \begin{pmatrix} \delta_1 \\ \vdots \\ \delta_{i-1} \\ \mathbf{d} \\ \delta_{i+1} \\ \vdots \\ \delta_{n-1} \end{pmatrix}. \quad (4.9)$$

We are essentially solving a version of system 4.5 in  $2n-3$  variables:  $\delta_1^T, \dots, \delta_{i-1}^T, \delta_{i+1}^T, \dots, \delta_{n-1}^T$ , each with two coordinates, and  $f$ .

**Theorem 2.** *Given a displacement  $\mathbf{d} = (d_x, d_y)^T$  of the moving finger, the displacement field  $\Delta'$  of the object and the squeezing force  $\mathbf{F}'$  are uniquely determined.<sup>2</sup>*

*Proof.* Denote  $\mathbf{u}'_j = (u'_{0,j}, \dots, u'_{2n-3,j})^T$ , for  $0 \leq j \leq 2n-3$ . Left multiply both sides of Equation 4.5, after substitution of Equation 4.7, by  $\mathbf{u}'_0{}^T, \dots, \mathbf{u}'_{2n-4}{}^T$  sequentially, utilizing the orthogonality of these vectors:

$$\begin{pmatrix} \lambda'_0 \mathbf{u}'_0{}^T \\ \vdots \\ \lambda'_{2n-4} \mathbf{u}'_{2n-4}{}^T \end{pmatrix} \Delta' = -f \begin{pmatrix} u'_{2i-1,0} \\ \vdots \\ u'_{2i-1,2n-4} \end{pmatrix}.$$

With the above, we project  $\Delta'$  onto  $\mathbf{u}'_0{}^T, \dots, \mathbf{u}'_{2n-3}{}^T$ , denoting  $g = \mathbf{u}'_{2n-3}{}^T \Delta'$ ,

$$\Delta' = -f \sum_{j=0}^{2n-4} \frac{1}{\lambda'_j} u'_{2i-1,j} \mathbf{u}'_j + g \mathbf{u}'_{2n-3}. \quad (4.10)$$

Since  $\mathbf{u}'_{2n-3} = \mathbf{v}'_r / \|\mathbf{v}'_r\|$ , we have  $u'_{2i-1,2n-3} = p_{ix} = 0$ . Hence  $\|\mathbf{u}'_{2i-1}\|^2 = \sum_{j=0}^{2n-4} u'_{wi-1,j}{}^2 = 1$ .

Now, we look at the two equations in Equation 4.10 that involve  $\mathbf{d}$ :

$$d_x = -f \sum_{j=0}^{2n-4} \frac{1}{\lambda'_j} u'_{2i-1,j} u'_{2i-2,j} + g u'_{2i-2,2n-3}, \quad (4.11)$$

$$d_y = -f \sum_{j=0}^{2n-4} \frac{1}{\lambda'_j} u'_{2i-1,j}. \quad (4.12)$$

---

<sup>2</sup>Theorem given and proven by Yan-Bin Jia.



The sum in Equation 4.12 is positive because  $\lambda'_j > 0$  for  $0 \leq j \leq 2n - 4$ , and some  $u'_{2i-1,j} \neq 0$ .

We solve the above two equations:

$$f = -d_y / \left( \sum_{j=0}^{2n-4} \frac{1}{\lambda'_j} u'^2_{2i-1,j} \right), \quad (4.13)$$

$$g = \frac{1}{u'_{2i-2,2n-3}} (d_x - d_y \left( \sum_{j=0}^{2n-4} \frac{1}{\lambda'_j} u'_{2i-1,j} u'_{2i-2,j} \right) / \left( \sum_{j=0}^{2n-4} \frac{1}{\lambda'_j} u'^2_{2i-1,j} \right)). \quad (4.14)$$

Finally, plug  $f$  and  $g$  into Equation 4.10 to obtain  $\delta_1^T, \dots, \delta_{i-1}^T, \delta_{i+1}^T, \dots, \delta_{n-1}^T$ .  $\square$

Or equivalently, with the boundary conditions given by Equation 4.1, 4.4 and 4.8, the system 3.7 is uniquely solvable.

In the special case  $d_y = 0$ , the finger in contact with  $\mathbf{p}_i$  moves in the  $x$ -direction. It follows from Equation 4.13 and 4.14 that  $f = 0$  and  $g = d_x / u'_{2i-2,2n-3}$ . Plugging them into Equation 4.7, we can show that  $\Delta = (d_x / u'_{wi-2,2n-3}) \mathbf{u}_{2n-3}$ . Consequently, the object undergoes a pure rotation with no deformation.

## 4.2 Squeeze Grasp

To squeeze the object, one finger moves towards the other, or in our scenario,  $d_x = 0$ . We refer to  $d = -d_y > 0$  as the *squeezing distance*.

**Corollary 1.** *Under a squeeze grasp, the contact forces and displacements of all vertices scale with the squeezing distance  $d$ .*

*Proof.* This follows directly from substitutions of  $d_x = 0$  and  $d_y = -d$  into Equation 4.13 and 4.14, and from subsequent substitutions of the obtained  $f$  and  $g$  into Equation 4.10.  $\square$

The next corollary states that a squeeze makes no difference in the resulting deformation if the moving and still fingers switch their roles.

**Corollary 2.** *Squeezing with  $\mathbf{p}_i$  fixed while  $\mathbf{p}_0$  moving toward  $\mathbf{p}_i$  by a distance of  $d$  yields the same shape except under a translation of  $(0, d)^T$ .*

*Proof.* Suppose that the original squeeze with  $\mathbf{p}_0$  fixed and  $\mathbf{p}_i$  moving by  $(0, -d)^T$  under force  $\mathbf{F}$  results in a displacement field  $\delta$ . System 3.7 is satisfied by  $\mathbf{F}$  and  $\delta$  under the constraints

$\delta_0 = 0$  and  $\delta_i = (0, -d)^T$ . It must also be satisfied by  $\mathbf{F}$  and a new displacement  $\delta' = \delta + d \cdot \mathbf{v}_y$  since  $\mathbf{v}_y$  is in the null space of  $K$ . A result analogous to Theorem 2 can be easily established to ensure that  $\mathbf{F}$  and  $\delta'$  are the unique solution under the new constraints  $\delta'_0 = (0, d)^T$  and  $\delta'_i = 0$ . The deformed shape is the same as the one constrained by  $\delta_0 = 0$  and  $\delta_i = (0, -d)^T$ , except it is translated by  $(0, d)^T$ .  $\square$

In a squeeze grasp, two finger contacts stay on the same line all the time. According to Proposition 1 and 2, the equilibrium of the body is guaranteed. We yet have to see that whether slip will happen or not. One simple fact is that, no slip happens between two contact objects if the contact force stays inside the friction cone. If the force is right on the edge of the friction cone, it depends on the initial state of the two objects. If they are relatively still in the initial state, then still no slip happens. Since Proposition 2 says that the direction of the squeezing force is parallel to  $\overline{\mathbf{p}_i \mathbf{p}_j}$ , then if  $\overline{\mathbf{p}_i \mathbf{p}_j}$  stays inside the friction cones all the time, no slip will happen. It follows directly that no rotation about  $\mathbf{p}_j$  may happen either, because if it does, slip must happen at  $\mathbf{p}_i$ .

The orientation of the friction cone can be represented by the orientation of the contact tangent, which is decided by its neighbor vertices. For example, the tangent at  $\mathbf{p}_i$  is along the direction of  $\mathbf{p}_{i+1} - \mathbf{p}_{i-1}$  before deformation and  $\mathbf{p}_{i+1} - \mathbf{p}_{i-1} + \delta_{i+1} - \delta_{i-1}$  after deformation. According to Corollary 1,  $\delta_{i+1} - \delta_{i-1}$  scales with  $d$ . Thus the orientation of the tangent changes monotonically with  $d$ . So if no slip happens on original shape and the deformed shape with squeezing distance  $d$ , then no slip may happen for any deformed shape with squeezing distance that is less than  $d$ . This agrees with our experience that hard squeezes are more likely to cause slips on soft objects.

Since the squeezing force scales with  $d$ , it should not be too small that the squeezing force fails requirements for certain tasks, for example, picking the object up from the supporting plane. Meanwhile,  $d$  cannot be too large in order for the squeezing forces to stay in their respective contact friction cones, and for the resulting deformation to be small enough so that it is well described by the linear elasticity.

How large can  $d$  be? Linear elasticity theory does not tell us. It depends on the material,

the global shape of the object, the contact locations, etc. For simplification, we introduce a factor  $\phi \in (0, 1)$  and consider all squeezing distances  $d = \rho \|\mathbf{p}_i - \mathbf{p}_j\|$ , where  $\rho \in (0, \phi]$ , to cause small deformations<sup>3</sup>. We call  $\rho$  the relative squeezing depth.

**Definition 1.** *A finger placement  $\mathcal{G}(\mathbf{p}, \mathbf{q})$  on an object is an  $\rho$ -squeeze grasp if*

- 1) *the line segment  $\overline{\mathbf{p}\mathbf{q}}$  is inside the friction cones at  $\mathbf{p}$  and  $\mathbf{q}$ , and*
- 2) *after deformation due to the displacement of  $\mathbf{p}$  to  $\tilde{\mathbf{p}} = \mathbf{p} + \rho(\mathbf{q} - \mathbf{p})$ , the line segment  $\overline{\tilde{\mathbf{p}}\mathbf{q}}$  lies inside the friction cones at  $\tilde{\mathbf{p}}$  and  $\mathbf{q}$  of the deformed shape.*

### 4.3 Generalized Squeeze Grasp

Now consider the case where  $d_x \neq 0$ .  $\tilde{\mathbf{p}}_i$  is now off the line  $\mathbf{p}_i\mathbf{p}_j$ . Although the total force sum up to 0 according to Proposition 1, the two squeezing forces do not point to each other according to Proposition 2, which means that there is a torque and equilibrium is broken.

Is a grasp only possible when the action is exactly squeeze? Of course not. The above illusion is due to the limit of linear elasticity in modeling the real world, as shown in Figure 3.2.

Let us leave linear elasticity theory aside for the moment, and look at Figure 4.2. Shape 1 and Shape 2 are undeformed shapes only different by an angle  $\alpha$  in orientation. Shape 3 are deformed shape of shape 1 generated by displacing point  $a$  to point  $b$ , a pure squeeze. Shape 4 are deformed shape of shape 1 generated by displacing point  $a$  to point  $d$ , where  $|dq| = |bq|$  and  $d$  is on  $\overline{cq}$ . The four shapes share a point  $p$ . Now consider the deformed shape  $s$  of shape 2 generated by displacing point  $c$  to point  $d$ , which is a pure squeeze. Shape  $s$  is the same as shape 4 because shape 1 and 2 are the same, and the corresponding points of them are fixed at same locations. Now, since shape 3 and shape 4 are both deformed shape generated by a pure squeeze of the same distance from the same shape, they are also the same, except for a difference  $\alpha$  in orientation. So the displacement  $\overrightarrow{ab}$  and  $\overrightarrow{ad}$  generates the same resulting shape. On the other hand, the force exerted at  $d$  is along  $\overrightarrow{dq}$  since shape 4 can be generated from shape 2 by the same pure squeezing. So both the deformed shape 3 and 4, and the grasping forces

---

<sup>3</sup>We usually take  $\phi$  to be less than 20%.

exerted on them, are the same, except for an angle  $\alpha$  in orientation. Thus if displacement  $\vec{ab}$  could result in a grasp, so could  $\vec{ad}$ .

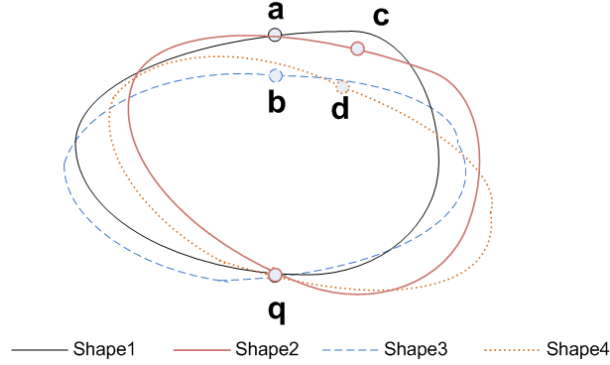


Figure 4.2: Generalized Squeeze Grasp. Shape 1 and Shape 2 are same undeformed shapes different by  $\alpha$  orientation.  $a$  and  $c$  are corresponding points. Shape 3 and Shape 4 are deformed shapes generated from shape 1 by displacement  $\vec{ab}$  and  $\vec{ad}$  resp. All 4 shapes share point  $q$ .  $a, b, q$  are collinear and  $c, d, q$  are also collinear.  $\|\vec{ab}\| = \|\vec{cd}\|$ .

**Proposition 3.** *If a finger placement  $\mathcal{G}(\mathbf{p}, \mathbf{q})$  can achieve a grasp by pure squeeze  $\mathbf{d}$  of  $\rho$ -depth, then any displacement  $\mathbf{d}'$  of the same squeeze depth can achieve a grasp. The set of all displacement vectors can be grouped into equivalent classes according to their squeeze depth at same finger placement.*

With above Proposition, given any finger placement and the displacement vector, we can test the grasp by testing the pure squeezing grasp at the same finger placement.

## CHAPTER 5. GRASP COMPUTATION

Algorithm 1 tests whether a general finger placement  $\mathcal{G}(\mathbf{p}_i, \mathbf{p}_j)$ ,  $0 \leq i < j \leq m - 1$  is a  $\rho$ -squeeze grasp. Step 4 of the algorithm is the most expensive one. A brute force method would fix one contact, say at  $\mathbf{p}_i$ , and solve system 4.5, where  $K'$  is the  $(2n - 2) \times (2n - 2)$  stiffness matrix generated after removing the  $2i$ -th and  $(2i + 1)$ -st rows and columns from  $K$ . Inversion of the matrix is necessary in order to check for different locations  $\mathbf{p}_j$  of the moving finger. This operation can be carried out in  $O(n^{2.807})$  time using Stassen's algorithm, or in  $O(n^{2.376})$  time using the Coppersmith-Winograd algorithm.<sup>1</sup>

---

**Algorithm 1** Test of  $\mathcal{G}(\mathbf{p}_i, \mathbf{p}_j)$  for a  $\rho$ -squeeze grasp

```

1: if  $\overline{\mathbf{p}_i \mathbf{p}_j}$  does not lie inside the friction cone at  $\mathbf{p}_i$  or  $\mathbf{p}_j$  then
2:   return no
3: else
4:   evaluate the tangents at  $\mathbf{p}_i$  and the displaced location  $\tilde{\mathbf{p}}_j$ , using  $\tilde{\mathbf{p}}_{i-1}$ ,  $\tilde{\mathbf{p}}_{i+1}$ ,  $\tilde{\mathbf{p}}_{j-1}$  and
      $\tilde{\mathbf{p}}_{j+1}$ 
5:   if  $\overline{\mathbf{p}_i \tilde{\mathbf{p}}_j}$  does not lie inside the friction cone at  $\mathbf{p}_i$  or  $\tilde{\mathbf{p}}_j$  then
6:     return no
7:   else
8:     return yes
9:   end if
10: end if

```

---

Nevertheless, the matrix  $K'$  changes whenever  $\mathbf{p}_i$  does, that is, whenever the still finger is relocated. A new matrix inversion needs to be performed. The number of matrix inversions equals  $m$ , the number of boundary vertices that are possible locations of  $\mathbf{p}_i$ . For a brute force iteration, the running time is  $O(m^2 n^{2.807})$  or  $O(n^{3.807})$  since  $m = O(\sqrt{n})$  for a solid object.

This chapter describes fast grasp testing that works on the stiffness matrix  $K$  only. We

---

<sup>1</sup>The latter algorithm is mainly useful for proving theoretical time bounds.

make use of its spectral decomposition 3.6, and obtain the matrices  $U$  and  $\Lambda$  via singular value decomposition (SVD) in  $O(n^3)$  time. Below we show that the placement  $\mathcal{G}(\mathbf{p}_i, \mathbf{p}_j)$  can be checked for a squeeze grasp in  $O(n)$  time.<sup>2</sup>

### 5.1 An Efficient Algorithm

Perform Singular Value Decomposition to the symmetric matrix  $K$

$$K = U\Sigma U^T, \quad (5.1)$$

where  $\Sigma = \text{diag}(\rho_0, \dots, \rho_{2n-4}, 0, 0, 0)$  with  $\rho_k$ 's being non-zero eigenvalues of  $K$ , and  $U = (\mathbf{w}_0, \dots, \mathbf{w}_{2n-1})^T$  is the orthonormal matrix consisting eigenvectors of  $K$  with  $\mathbf{w}_k$ 's being its row vectors written in column vector form.

Now apply the coordinate transformation. Let

$$\mathbf{y} = \begin{pmatrix} y_0 \\ \vdots \\ y_{2n-1} \end{pmatrix} = U^T \Delta. \quad (5.2)$$

Since  $U$  is orthonormal,  $U^T = U^{-1}$ . Then

$$\Delta = U\mathbf{y}. \quad (5.3)$$

Substitute it into Equation 3.7:

$$K\Delta = U\Sigma U^T U\mathbf{y} = U\Sigma\mathbf{y} = \mathbf{F},$$

Left multiply  $U^T$  on both sides of the last equal sign, we get

$$\begin{aligned} (\rho_0 y_0, \dots, \rho_{2n-4} y_{2n-4}, 0, 0, 0)^T &= U^T \mathbf{F} \\ &= U^T (0, \dots, 0, f_{2i}, f_{2i+1}, 0, \dots, 0, f_{2j}, f_{2j+1}, 0, \dots)^T \\ &= f_{2i} \mathbf{w}_{2i} + f_{2i+1} \mathbf{w}_{2i+1} + f_{2j} \mathbf{w}_{2j} + f_{2j+1} \mathbf{w}_{2j+1}. \end{aligned} \quad (5.4)$$

---

<sup>2</sup>The efficient algorithm was mainly developed by Yan-Bin Jia and Huan Lin

Let  $\mathbf{r} = (r_x, r_y)^T = (\mathbf{p}_j - \mathbf{p}_i) / \|\mathbf{p}_j - \mathbf{p}_i\|$ . According to Proposition 1 and 2,

$$\begin{pmatrix} f_{2i} \\ f_{2i+1} \\ f_{2j} \\ f_{2j+1} \end{pmatrix} = f \begin{pmatrix} \mathbf{r} \\ -\mathbf{r} \end{pmatrix},$$

where  $f$  is the magnitude of the force. Let  $\mathbf{a} = (\mathbf{r}^T, -\mathbf{r}^T)^T$  and  $W = (\mathbf{w}_{2i}, \mathbf{w}_{2i+1}, \mathbf{w}_{2j}, \mathbf{w}_{2j+1})$ ,

Equation 5.4 becomes

$$\begin{pmatrix} \rho_0 y_0 \\ \vdots \\ \rho_{2n-4} y_{2n-4} \\ 0 \\ 0 \\ 0 \end{pmatrix} = f W \mathbf{a}.$$

Divide the  $i$ -th entry of both sides of the above equation by  $\rho_i$ , for  $0 \leq i \leq 2n - 4$ , resp., and denote the resulting vector of the right side as  $P$ , we get:

$$\begin{pmatrix} y_0 \\ \vdots \\ y_{2n-4} \\ 0 \\ 0 \\ 0 \end{pmatrix} = f P. \tag{5.5}$$

Since  $\Delta = U\mathbf{y}$ ,

$$\begin{aligned}
(\delta_i^T, \delta_j^T)^T &= W^T \mathbf{y} \\
&= W^T \left[ \begin{pmatrix} y_0 \\ \vdots \\ y_{2n-4} \\ 0 \\ 0 \\ 0 \end{pmatrix} + \begin{pmatrix} 0 \\ \vdots \\ 0 \\ y_{2n-3} \\ y_{2n-2} \\ y_{2n-1} \end{pmatrix} \right] \\
&= fW^T P + W_{s3}^T \begin{pmatrix} y_{2n-3} \\ y_{2n-2} \\ y_{2n-1} \end{pmatrix}. \tag{5.6}
\end{aligned}$$

where  $W_{s3}$  is a  $3 \times 4$  submatrix of  $W$  taking its last 3 rows. Given  $(\delta_i^T, \delta_j^T)^T = (0, 0, \mathbf{d}^T)^T$ , we then have

$$\begin{pmatrix} W^T P & W_{s3}^T \end{pmatrix} \begin{pmatrix} f \\ y_{2n-3} \\ y_{2n-2} \\ y_{2n-1} \end{pmatrix} = \begin{pmatrix} 0 \\ 0 \\ \mathbf{d} \end{pmatrix}. \tag{5.7}$$

Once we solve the above 4 by 4 system, we can calculate  $\mathbf{y}$  using Equation 5.5. And then  $\Delta$  is solved using Equation 5.3.

## 5.2 Algorithm Analysis

The preprocessing, SVD, takes  $O(n^3)$  time. After the that, obtaining  $W^T P$  takes  $O(n)$  time, and obtaining  $W_{s3}^T$  takes constant time. Solving the system 5.7 takes constant time. Obtaining  $\mathbf{y}$  takes  $O(n)$  time. With  $\mathbf{y}$ , we can evaluate any value of  $\Delta$  in  $O(n)$  time.

Get Back to step 4 of Algorithm 1, evaluating  $\tilde{\mathbf{p}}_{i-1}$ ,  $\tilde{\mathbf{p}}_{i+1}$ ,  $\tilde{\mathbf{p}}_{j-1}$  and  $\tilde{\mathbf{p}}_{j+1}$ , which takes  $O(n)$  time, gives us the result of one grasp testing.

**Theorem 3.** *After SVD of the stiffness matrix  $K$ , which takes  $O(n^3)$  time, the grasp test on a finger placement  $\mathcal{G}(\mathbf{p}_i, \mathbf{p}_j)$  takes  $O(n)$  time.*



To compute the global deformation resulted by one grasp, we need to evaluate  $\Delta$ , which takes  $O(n^2)$  time, or, if we only need the contour of the shape,  $2m-4$  entries of  $\Delta$  are evaluated, which takes  $O(n^{1.5})$  time. To find all grasps, we exhaustively test the  $\binom{m}{2}$  pairs of boundary points, which can be done in  $O(m^2n)$ , or  $O(n^2)$  time. The overall running time is dominated by SVD.

Table 5.1 shows the running time of the naive algorithm and the efficient algorithm for different tasks on solid and hollow objects<sup>3</sup>. We can see that almost for every task, the efficient algorithm reduces the time by order of 2.

Table 5.1: Algorithm Comparison. Running time of naive and efficient algorithms on different tasks and different types of object.

	Naive		Efficient(after SVD $O(n^3)$ )	
	Solid	Hollow	Solid	Hollow
Single Grasp Test	$O(n^3)$	$O(n^3)$	$O(n)$	$O(n)$
Compute global deformed contour	$O(n^3)$	$O(n^3)$	$O(n^{1.5})$	$O(n^2)$
Find 2nd finger location given 1st	$O(n^{3.5})$	$O(n^4)$	$O(n^{1.5})$	$O(n^2)$
Find all grasps	$O(n^4)$	$O(n^5)$	$O(n^2)$	$O(n^3)$

---

<sup>3</sup>Hollow objects are the object with all the elements on the boundary. More detailed description will be seen in Chapter 6

## CHAPTER 6. ROBOT EXPERIMENT

Figure 6.1 shows the experimental setup in which grasping was carried out by two fingers of a Barrett Hand. Every finger had a strain gauge sensor mounted at its lower joint to measure contact force.



Figure 6.1: Grasping with a Barrett Hand.

The hand initially grasped two hollow objects displayed in the first column of Table 6.1. They were cut from food and medicine containers, respectively. Such an object could be viewed as one swept out by a rectangular cross section with width  $w$  and height  $h$  along a closed 2-D curve  $\gamma(s)$  parametrized by arc length  $s$  and having length  $L$ . Let the displacement field along the curve be  $\delta(s) = \alpha(s)\mathbf{t} + \beta(s)\mathbf{n}$ , where  $\mathbf{t}$  and  $\mathbf{n}$  are the unit tangent and normal on the curve. The strain energy takes the form (9):

$$U_c = \frac{1}{2}Ew \int_0^L \left( h\epsilon^2 + \frac{h^3}{12}\zeta^2 \right) ds, \quad (6.1)$$

with the extensional strain  $\epsilon = d\alpha/ds - \kappa\beta$  and the change  $\zeta = -d^2\beta/ds^2 - (d\kappa/ds)\alpha - \kappa(d\alpha/ds)$  in the curvature  $\kappa$ . Under the FEM scheme, all elements lie on the boundary. The strain energy  $U_c$  can be written in the form of 3.3 with a semi-positive stiffness matrix. We can show that

the analytical results from Chapters 3 and 4 carry over.

The elliptic object in Table 6.1 was made of high-density polyethylene (Young’s modulus  $E = 0.8\text{GPa}$ ), and the triangle-like object was made of polyethylene terephthalate ( $E = 3\text{GPa}$ ). Their cross sections had sizes  $11\text{mm} \times 0.6\text{mm}$  and  $20\text{mm} \times 0.6\text{mm}$ , respectively. The surfaces of the objects were filed to increase friction with fingers. The coefficients of friction were measured by determining the max slope of the phalange on which the objects could be placed without slip. The values were 0.9 for the elliptic ring and 0.6 for the triangular one. The second column of Table 6.1 shows the simulation results of two grasps, and the third column shows the outcomes of an experiment (which matched the simulation results well), both at 10%-squeeze depth.

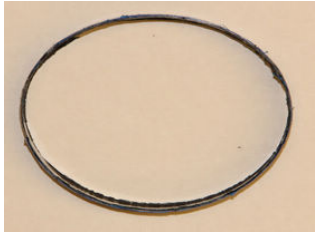
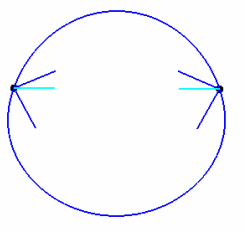


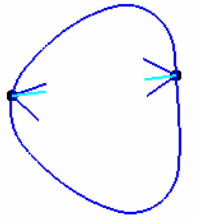

Shape	Simulation	Experiment
		
		

Table 6.1: Grasping two ring-like objects (column 1): simulation (column 2) and experimental (column 3).

Figure 6.2 shows the graspable regions of the 3 objects. The graspable regions grow significantly with the friction coefficient. However, they decrease very little while  $w$  increases from 1% to 10%. Note that the regions are symmetric about line  $y = x$ , as implied by Corollary 2.

Figure 6.3 shows simulation results on graspable regions with  $\mu = 0.5$ . The black segments in Figure 6.3(a) represent a pair of independent graspable regions of the object at 10% squeeze depth. Two fingers may be placed at any one point from each region and form a grasp at

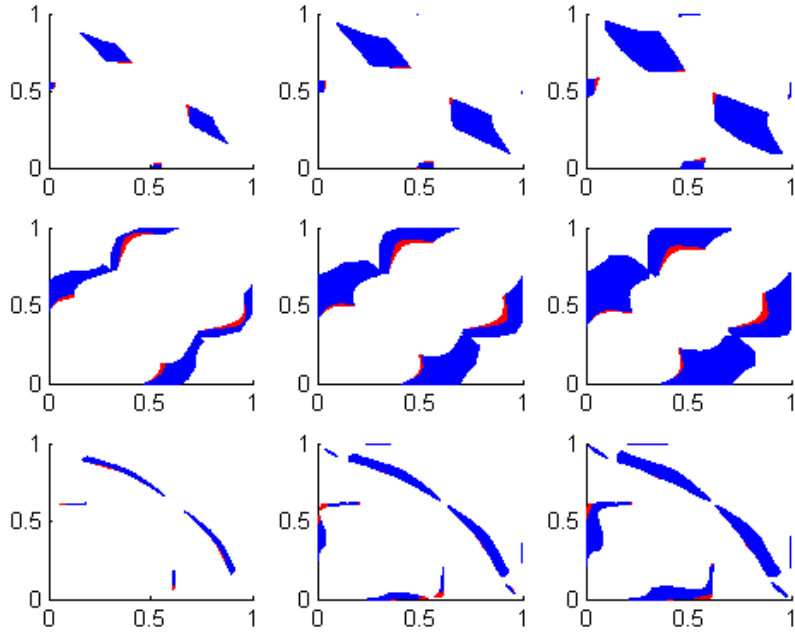


Figure 6.2: Graspable regions. Cell  $(i, j)$ ,  $i, j = 1, 2, 3$ , shows the graspable regions on object  $i$  with friction coefficient  $\mu_j = 0.3, 0.5, 0.7$ , resp. The blue regions are 10%–graspable and also 1%–graspable, and the red regions are only 1%–graspable.

10% squeeze depth. In Figure 6.3(b), the colored regions represent the set of all the location pairs that form grasps at 10% squeeze depth. The red rectangular in 6.3(b) corresponds to the independent graspable regions shown in 6.3(a).

Next, the hand grasped solid objects of rubber foam ( $E = 50\text{KPa}$ , Poisson’s ratio  $\nu = 0.3$  and coefficient of friction  $\mu = 1.3$ ). Shown in Figure 6.4 are two instances of grasping an object with the longest diameter 10.4cm and thickness 2.56cm.

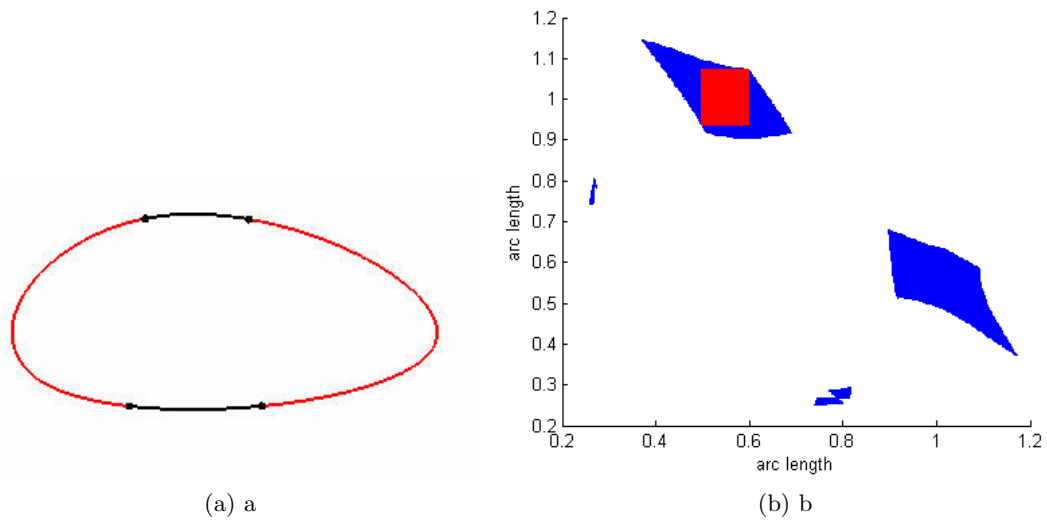


Figure 6.3: (a) Independent graspable segments (colored in black) for the relative squeeze depth of  $s = 10\%$ ; and (b) the set of grasps, each represented as a point with its coordinates indicating the arc length values of the two contact positions. The red rectangular region in (b) corresponds to the pair of black segments in (a) on which two fingers can be placed independently to form a grasp.

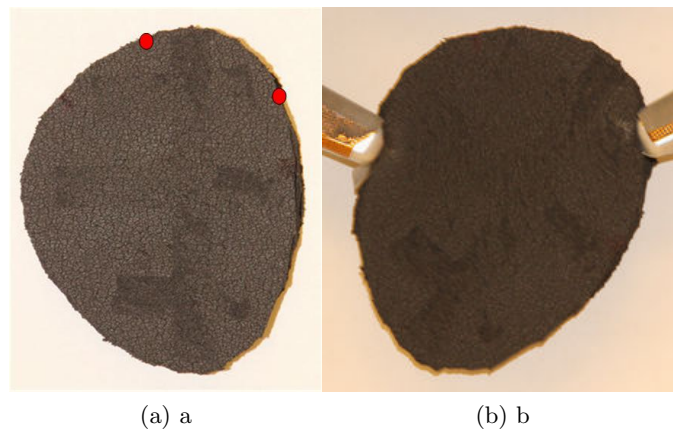


Figure 6.4: Grasping a foam object: (a) underdeformed shape and (b) grasp configuration. The pair of points in (a) marks an unsuccessful grasp.

## CHAPTER 7. DISCUSSION

This thesis studies how to grasp planar deformable objects by squeezing them with two point fingers. The key idea is to specify desired finger displacements rather than forces, and to use them as constraints over an object so that its deformed shape can be computed and checked for equilibrium after deformation. We have conducted an analysis of this method and developed an efficient algorithm to find all grasps (up to discretization under the finite element scheme).

Specification of finger displacements over finger forces not only makes the strategy close to a real grasping scenario, but also helps stabilize the grasp. If constant forces are specified, grasping would act like an inverted pendulum and have no resistance to disturbance intended to cause rotation. If finger displacements are specified, however, disturbances up to certain magnitude can be resisted by friction at two contacts.

The 5th assumption ignores the dynamics in grasping and only look at the start and finish of the process. Assuming quasi-static process may also ignore dynamics, yet allows us to study the internal process. The concept of finger displacement can be replaced by the path of the moving finger, which specifies a bigger problem set.

Future work may include grasp stability, area finger contacts and grasping 3-dimensional deformable objects.

**BIBLIOGRAPHY**

- [1] A. Bicchi and V. Kumar, “Robotic grasping and contact: a review,” in *Proc. IEEE Intl. Conf. Robot. Autom.*, 2000, pp. 348–353.
- [2] A. Blake, “A symmetry theory of planar grasp,” *Int. J. Robot. Res.*, vol. 14, pp. 425–444, 2004.
- [3] S.H. Crandall, N.C Dahl, T.J. Lardner, “An Introduction to the Mechanics of Solids”, 2nd edition, McGraw-Hill, pp. 302, 1978.
- [4] Y.-C. Fung, P. Tong, “Classical and Computational Solid Mechanics” *World Scientific*, pp. 280–281, 2001.
- [5] R.H. Gallagher, “Finite Element Analysis: Fundamentals”, Prentice-Hall, Englewood Cliffs, N.J., 1975.
- [6] K. Gopalakrishnan and K. Goldberg, “D-space and deform closure grasps of deformable parts,” *Int. J. Robot. Res.*, vol. 24, pp. 899–910, 2005.
- [7] S. Hirai, T. Tsuboi, and T. Wada, “Robust grasping manipulation of deformable objects,” in *Proc. IEEE Symp. Assembly and Task Planning*, 2001, pp. 411-416.
- [8] Y.-B. Jia, “Computation on parametric curves with an application in grasping,” *Int. J. Robot. Res.*, vol. 23, pp. 825–855, 2004.
- [9] Y.-B. Jia, F. Guo, J. Tian, “On two-finger grasping of deformable planar objects,” *IEEE Intl. Conf. Robot. Autom.*, 2011, pp. 5261–5266.

- [10] Q. Luo and J. Xiao, "Geometric properties of contacts involving a deformable object," in *Proc. IEEE Symp. Haptic Interfaces Virtual Env. Tele. Sys.*, 2006, pp. 533–538.
- [11] B. Mirtich and J. Canny, "Easily computable optimum grasps in 2-D and 3-D," in *Proc. IEEE Int. Conf. Robot. Autom.*, 1994, pp. 739–747.
- [12] B. Mishra and M. Teichmann, "Three finger optimal planar grasps," in *Proc. IEEE/RSJ Int. Conf. Intell. Robots and Systems*, 1994.
- [13] V. D. Nguyen, "Constructing force-closure grasps," *Int. J. Robot. Res.*, vol. 7, pp. 3–16, 1988.
- [14] J. Ponce, S. Sullivan, J.-D. Boissonnat, and J. P. Merlet, "On characterizing and computing three- and four-finger force-closure grasps of polyhedral objects," in *Proc. IEEE Int. Conf. Robot. Autom.*, 1993, pp. 821–827.
- [15] J. Ponce, D. Stam, and B. Faverjon, "On computing two-finger force-closure grasps of curved 2D objects," *Int. J. Robot. Res.*, vol. 12, pp. 263–273, 1993.
- [16] Sinha, P.R.. Abel, J.M., "Acontact stress model for multifingerd grasps of rough objects," *IEEE Trans. on Robot. and Autom.*
- [17] G. Strang, "Introduction to Linear Algebra", en edition, Wellesly-Cambridge Press, pp.273, 1993
- [18] J. Tian and Y.-B. Jia, "Modeling deformable general parametric shells grasped by a robot hand," scheduled to appear in *IEEE Trans. on Robot.*, vol. 26, 2010.
- [19] H. Wakamatsu, S. Hirai and K. Iwata, "Static analysis of deformable object grasping based on bounded force closure," in *Proc. IEEE/RSJ Intl. Conf. Intell. Robots and Systems*, 1996, pp. 3324–3329.
- [20] H. Wakamatsu and S. Hirai, "Static modeling of linear object deformation based on differential geometry," *Int. J. Robot. Res.*, vol. 23, pp. 293–311,2004.